Applied Thermal Engineering 161 (2019) 114188

Contents lists available at ScienceDirect

Applied Thermal Engineering

journal homepage: www.elsevier.com/locate/apthermeng

Research Paper

Globally optimal design of air coolers considering fan performance

Carolina B. Carvalho[a], Mauro A.S.S. Ravagnani[a], Miguel J. Bagajewicz[b], André L.H. Costa[c,*]

[a] State University of Maringá (UEM), Chemical Engineering Department, Avenida Colombo, 5790, Maringá, PR CEP 87020-900, Brazil
[b] School of Chemical, Biological and Materials Engineering, University of Oklahoma, Norman, OK 73019, USA
[c] Institute of Chemistry, Rio de Janeiro State University (UERJ), Rua São Francisco Xavier, 524, Maracanã, Rio de Janeiro, RJ CEP 20550-900, Brazil

HIGHLIGHTS

- An air cooler model is presented, including the fan selection in the formulation.
- The resulting model is a mixed integer nonlinear programming (MINLP) problem.
- The global optimum is found employing enumerative search schemes.

ARTICLE INFO

Keywords:
Optimization
Design
Air coolers

ABSTRACT

Design optimization of air coolers is often presented limiting fan calculations to the required power, without considerations of fan capabilities or commercial viability. In this article, new design optimization procedures are presented to include the selection of a commercial-type fan and, thus, the air flow rate as a variable. The resulting model is a mixed integer nonlinear programming (MINLP) problem, which is solved globally, using three different enumeration procedures, and the performance among them is compared. The proposed approaches are illustrated by two case studies. Results showed that the smart enumeration scheme can provide the global solution in an acceptable computational time even when considering large problems.

1. Introduction

Air coolers are heat exchangers composed of one or more banks of finned tubes that are employed to transfer heat from a hot stream to atmospheric air, usually using fans to promote the air flow. Considering environmental concerns such as potential water shortage problems and regions where the available water requires expensive treatments, air coolers can be an important option in relation to conventional water coolers.

The published papers that addressed the design and optimization of air coolers are based on two main approaches: meta-heuristic methods and mathematical programming.

Regarding the utilization of meta-heuristic techniques, Doodman et al. [1] used the global sensitive analysis to investigate the influence of the design parameters on the total cost of air coolers. The analysis resulted in the exclusion of the number of fins and tube passes from the optimization step performed by the harmonic search algorithm. The annual total cost was slightly reduced when compared to other meta-heuristic techniques. The design parameters of the heat exchanger itself were also investigated using the imperialist competitive algorithm [2,3] to enhance the global heat transfer coefficient of the equipment. In another approach, a multi-objective optimization problem was formulated to find the optimal geometric design of an air cooler by using the genetic algorithm [4] and an extensive discussion about the influence of the geometry characteristics and the temperature approach (tube side fluid outlet and air inlet temperatures) in the annual total cost was provided by the authors.

The application of mathematical programming for the design and optimization of air coolers contemplated different techniques: nonlinear programming (NLP) [5], mixed-integer nonlinear programming (MINLP) [6], mixed-integer linear programming (MILP) and integer linear programming (ILP) [7].

The environmental effects inherent to air coolers are also a topic of interest regarding their performance and optimization, such as wind conditions [8], air temperature rise [9], freezing conditions due to severe winter [10], fan load factor [11], and heat load variation [12]. In addition, the air cooler performance during wet and dry air conditions were experimentally investigated and compared with the correlations from literature, revealing smaller differences for dry operations [13].

Innovative design configurations were proposed to overcome some

* Corresponding author.
E-mail address: andrehc@uerj.br (A.L.H. Costa).

https://doi.org/10.1016/j.applthermaleng.2019.114188
Received 5 February 2019; Received in revised form 12 June 2019; Accepted 26 July 2019
Available online 03 August 2019
1359-4311/

Nomenclature

Parameters

$\widehat{CRF}$	annualization factor
$\hat{f}d$	minimum distance between the fan and the bay width (m)
$\hat{f}l$	minimum distance between the fan and the bay length (m)
$\hat{g}$	gravitational acceleration (m/s^2)
$\hat{k}t$	tube thermal conductivity (W(/m·K))
$\hat{p}$	pressure (Pa)
$\widehat{P}rh$	hot stream Prandtl number
$\widehat{Q}$	heat load (W)
$\widehat{R}fc$	air stream fouling factor (m^{2}K/W)
$\widehat{R}fh$	Hot stream friction factor (m^{2}K/W)
$\widehat{T}ci$	air inlet temperature (°C)
$\hat{v}hmax$	maximum allowable tube side flow velocity (m/s)
$\hat{v}hmin$	minimum allowable tube side flow velocity (m/s)
$\widehat{X}a$	excess of area
$\hat{z}$	elevation (m)
$\widehat{\alpha t}$	minimum spacing between the fins of adjacent tubes (m)
$\widehat{\Delta Phmax}$	maximum allowable tube side pressure drop (Pa)
$\hat{\eta}motor$	motor efficiency
$\hat{\eta}sr$	speed reducer efficiency
$\widehat{\rho h}$	hot stream density (kg/m^3)

Variables

A	heat transfer area (m^2)
Aot	total finned surface area per unit length (m^2/m)
Ar	outside tube bare area per unit length (m^2/m)
$Areq$	required heat transfer area (m^2)
$Cinv$	capital cost ($)
$Cmai$	yearly maintenance cost ($/year)
Cop	operational cost ($/year)
Cpc	air heat capacity (J/(kg·K))
$Dfan$	Fan diameter (m)
Dte	tube outer diameter (m)
Dti	inner tube diameter (m)
F	LMTD correction factor
Gh	mass flux of the hot stream (kg/m^{2}s)
Ltp	tube pass (m)
fc	air friction factor (dimensionless)
hc	air stream heat transfer coefficient (W/(m^{2}K))
hh	hot stream heat transfer coefficient (W/(m^{2}K))
L	tube length (m)
Lf	fin height (m)
$Lfanp$	distance between the fan centers (m)
Ltp	tube pitch (m)
mc	air mass flow rate (kg/s)
$Nbay$	number of bays
$Nbbay$	number of bundles per bay
Nf	number of fins per tube length (1/m)
$Nfanbay$	number of fans per bay
Nr	number of tube rows
Ntr	number of tubes per row
Prc	air stream Prandtl number (dimensionless)
Nuc	air stream Nusselt number (dimensionless)
Nuh	hot stream Nusselt number (dimensionless)
$qfan$	air volumetric flow rate per fan (m^3/s)
Rec	air stream Reynolds number (dimensionless)
Reh	hot stream Reynolds number (dimensionless)
Tc	air temperature (°C)
TAC	total annualized cost ($/year)
Tco	air outlet temperature (°C)
U	overall heat transfer coefficient (W/(m^{2}K))
vc	air flow velocity (m/s)
$\dot{w}_{fan}$	energy per unit of volume (J/m^3)
W	bundle width (m)
$\dot{W}_{fan}$	individual fan power (W)
$\dot{W}_{motor}$	motor power (W)
ΔPf	pressure drop of the hot stream in the tubes (Pa)
ΔPh	total pressure drop of the hot stream (Pa)
ΔPr	pressure drop of the hot stream in the exchanger heads (Pa)
ΔTlm	logarithmic mean temperature difference (LMTD) (°C)
ηt	overall efficiency of the finned surface
ηfan	fan efficiency
ρ	air density (kg/m^3)

Subscripts

apc	air plenum chamber
avg	average conditions between inlet and outlet air flow
i	inlet
o	outlet

of these environmental issues, such as a bilaterally arranged system to minimize wind impacts [14], a novel vertical layout using the wind to improve the thermo-flow performance [15] and the installation of windbreak walls [16].

The typical formulation of the design optimization problem is composed of capital and operational costs. Capital costs include the investment associated to the tube bundles, bays structure and fans. Operational costs represent the energy consumption associated to fan operation.

In all previous works cited, no matter the solution technique employed, it is considered that the power needed to drive the fan is a direct function of the air-side pressure drop, ignoring the fact that the air flow rate and the pressure drop are consequence of the hydraulic interaction between the tube bundles and the fan, i.e. a mechanical energy balance involving the fan curve and the system curve.

Despite the efforts to address the design problem in the most realistic operational conditions, in the majority of the cases the designed unit will have to be adapted to what is available from manufacturers [5], which may depart from the final solution. Therefore, the outcome may be a suboptimal design with higher costs than those determined by the optimization.

Aiming at filling this gap, this paper presents the optimization of air coolers considering the fan performance, where the selection of the fan is a design variable and the corresponding air flow rate is the result of a mechanical energy balance. This approach allows an accurate solution, represented by the air cooler tube bundle and bays as well as fans, without the need of any rounding up procedure to identify a suitable fan to be applied after the optimization, as it is used implicitly in all previous approaches.

Aiming at overcoming the issues related to the nonlinearities of a MINLP in finding the global optimal solution using typical mathematical programming techniques, this paper proposes different variants of enumeration procedures to find the global solution in an acceptable execution time.

2. Air cooler model

The thermal model for both streams and the hot stream flow model are composed of the same equations employed by Souza et al. [7], according to Serth [17] (see Supplementary Material). The optimization

including the air flow model proposed below is a new contribution of this paper. Aiming at making the presentation easier to the reader, the parameters are differentiated from the variables using the symbol "^" over them.

2.1. Air flow model

There are two options of air cooler configurations: forced draft (Fig. 1a) and induced draft (Fig. 1b). Air coolers consisting of a set of bays (*Nbay*), where each bay is built using one or more tube bundles (*Nbbay*), associated to a number of fans per bay (*Nfanbay*) are considered. Fig. 1c shows an example of a bank with three bays ($Nbay = 3$), each composed of two tube bundles ($Nbbay = 2$) associated to two fans ($Nfanbay = 2$). In turn, Fig. 1d shows a bank with two bays ($Nbay = 2$) composed of two tube bundles ($Nbbay = 2$) associated to one fan ($Nfanbay = 1$).

The mechanical balance of the overall fan-tube bundles structure is given by:

$$\hat{\rho}_i\left(\frac{v_{ci}^2}{2}+\frac{\hat{p}_i}{\hat{\rho}_i}+\hat{z}_i\hat{g}\right)=\rho_o\left(\frac{v_{co}^2}{2}+\frac{\hat{p}_o}{\rho_o}+\hat{z}_o g\right)-\dot{w}_{fan}+2.2\rho_{avg}f_c v_{cavg}^2 Nr \tag{1}$$

The last term is the friction loss across the tube bundles [17].

The relation between the inlet and outlet air temperatures is given by:

$$Tco=\hat{T}ci+\frac{\hat{Q}}{Cpcmc} \tag{2}$$

where *mc* is the air mass flow rate which has the following relationship with the total air volumetric flow rate entering the fans (q_{air}) at the corresponding inlet temperature $\hat{T}ci$ or Tco, depending of the case:

$$mc=\begin{cases} q_{air}\rho_o & \text{for induced draft}\\ q_{air}\hat{\rho}_i & \text{for forced draft}\end{cases} \tag{3}$$

The volumetric flow rate corresponding to each fan is given by:

$$q_{fan}=\frac{q_{air}}{NbayNfanbay} \tag{4}$$

The potential energy difference, that is, $g(\rho_o z_o-\hat{\rho}_i z_i)$, is usually neglected, and $p_i=p_o=p_{atm}$ (atmospheric pressure) and $v_{ci}=0$. Multiplying the expression of $\dot{w}_{fan}$ from Eq. (1) by the fan volumetric flow rate, one gets the power needed per fan (BHP):

$$\dot{W}_{fan}=\frac{\left(\rho_o\frac{v_{co}^2}{2}+2.2\rho_{avg}f_{cv}v_{avg}^2 Nr\right)q_{fan}}{\eta_{fan}} \tag{5}$$

This expression is valid for air coolers based on induced and forced draft. The flow velocity at the outlet (v_{co}) is equal to the velocity at the tube bundle for forced draft, and equal to the fan velocity for induced draft, although, it is a common practice to consider v_{co} equal to the fan velocity in both cases [17].

The corresponding energy consumption per motor ($\dot{W}_{motor}$) is then obtained by dividing $\dot{W}_{fan}$ by the speed reducer efficiency ($\hat{\eta}sr$) and the motor efficiency ($\hat{\eta}motor$):

$$\dot{W}_{motor}=\frac{\dot{W}_{fan}}{\hat{\eta}sr\hat{\eta}motor} \tag{6}$$

Without loss of generality, we now focus on the forced draft type. The fan curve represents the pressure increase through the fan, from atmospheric pressure to the pressure of the air plenum chamber, the region between the fan and the bundles of tubes:

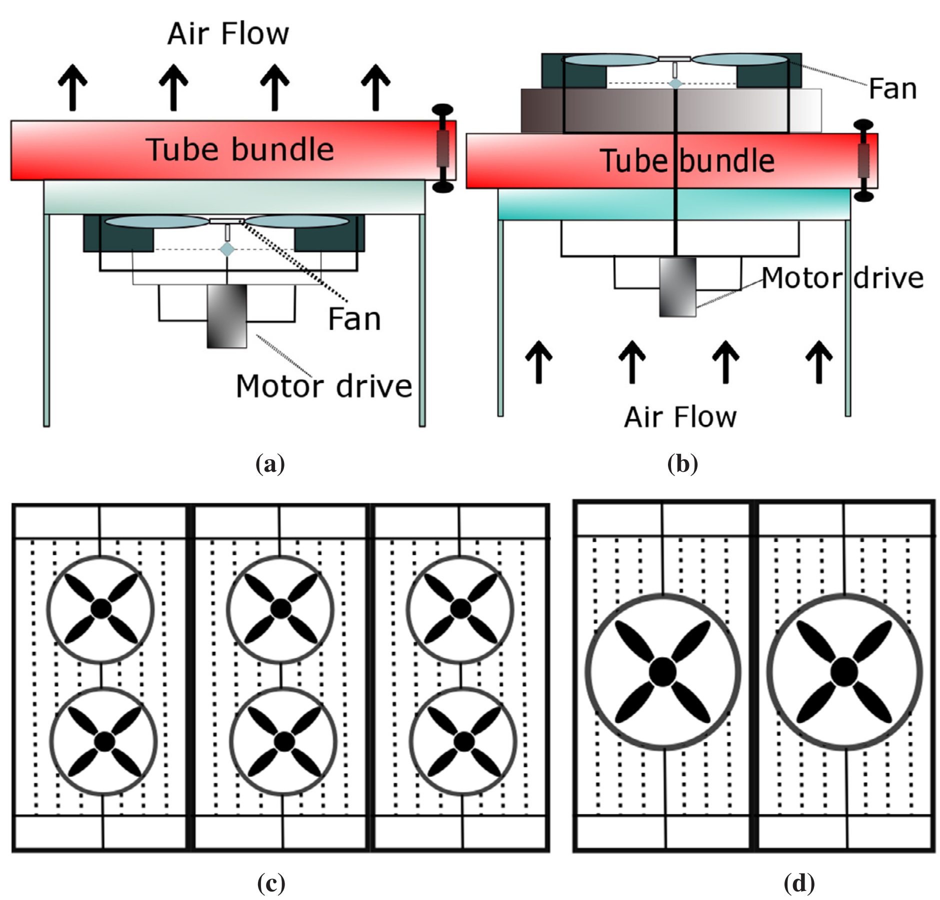

Fig. 1. Air cooler alternatives: (a) Forced draft, (b) Induced draft, (c) A bank with three bays, two bundles per bay and two fans per bay, (d) A bank with two bays, two bundles per bay and one fan per bay.

$$(p_{apc} - p_i) = g_{fan}(q_{fan}) \tag{7}$$

Here, the fan curve in Eq. (7) uses static pressures, but the literature also contains representations of the fan curves in relation to the total pressure, i.e. the sum of static and dynamic pressures. The function $g_{fan}(q_{fan})$ can be represented by a polynomial fit to the manufacturer's curve. In turn, the tube bundle curves represent the pressure drop across the tube bundles ("system curve"). Fig. 2 depicts these curves and also the BHP curve, that is the brake-horse power of the fan, which can be used instead of Eq. (5), when available.

The system curve is obtained using the mechanical energy balance between the air plenum chamber and the bundle outlet:

$$\hat{\rho}_i\left(\frac{v_{capc}^2}{2} + \frac{p_{apc}}{\hat{\rho}_i} + z_i g\right) = \rho_o\left(\frac{v_{co}^2}{2} + \frac{p_o}{\rho_o} + z_o g\right) + 2.2\rho_{avg} f_c v_{cavg}^2 Nr \tag{8}$$

Neglecting the potential energy changes, and rearranging to get the pressure drop, we get:

$$(p_{apc} - p_o) = \left(\rho_o \frac{v_{co}^2}{2} - \hat{\rho}_i \frac{v_{capc}^2}{2}\right) + 2.2\rho_{avg} f_c v_{cavg}^2 Nr \tag{9}$$

Thus, the flowrate where both curves cross is the root of the equation relating Eq. (9) and Eq. (7), i.e. $(p_{apc} - p_i) = (p_{apc} - p_o)$, which becomes:

$$g_{fan}(q_{fan}) = \left(\rho_o \frac{v_{co}^2}{2} - \hat{\rho}_i \frac{v_{capc}^2}{2}\right) + 2.2\rho_{avg} f_c v_{cavg}^2 Nr \tag{10}$$

Without loss of generality, a third-degree polynomial to represent the fan curve is used. In addition, the term $\left(\rho_o \frac{v_{co}^2}{2} - \hat{\rho}_i \frac{v_{capc}^2}{2}\right)$ is neglected because it is substantially smaller than the friction losses. As a result, one obtains

$$[\widehat{AP}_{fan} + \widehat{BP}_{fan} q_{fan} + \widehat{CP}_{fan} q_{fan}^2 + \widehat{DP}_{fan} q_{fan}^3] = 2.2\rho_{avg} f_c v_{avg}^2 Nr \tag{11}$$

After $f_c v_{avg}^2$ is expressed in terms of q_{fan}, one solves Eq. (11) to obtain q_{fan}. For fans with induced draft, the calculations are slightly different, where after some simplifications, one can arrive at the same expression.

2.2. Hot stream flow model

The tube side pressure drop (ΔPh) encompasses the pressure drops through the tubes (ΔPf) and heads (ΔPr) (See Supplementary Material):

$$\Delta Ph = \Delta Pf + \Delta Pr \tag{12}$$

The total tube-side pressure drop is constrained by the maximum allowed value:

$$\Delta Ph \le \Delta \widehat{Phmax} \tag{13}$$

Additionally, tube-side flow velocity bounds are also imposed:

$$\hat{v}hmin \le \frac{Gh}{\hat{\rho} h} \le \hat{v}hmax \tag{14}$$

2.3. Thermal model

The convective coefficients of the hot and cold streams are evaluated by (see Supplementary Material for more details):

$$Nuh = 0.023Reh^{0.8}\hat{P}rh^{\frac{1}{3}} \tag{15}$$

$$Nuc = 0.38Rec^{0.6}Prc^{\frac{1}{3}}\left(\frac{Aot}{Ar}\right)^{-0.15} \tag{16}$$

Therefore, the overall heat transfer coefficient (U) can be calculated by:

$$U = \frac{1}{\left(\frac{1}{hh} + \hat{R}fh\right)\left(\frac{Aot}{\pi Dti}\right) + \left[\frac{Aot\ln\left(\frac{Dte}{Dti}\right)}{2\pi\hat{k}t}\right] + \frac{1}{\eta thc} + \frac{\hat{R}fc}{\eta t}} \tag{17}$$

The required heat transfer area ($Areq$) is calculated using the LMTD method:

$$Areq = \frac{\hat{Q}}{U\Delta TlmF} \tag{18}$$

For a reliable design, the total heat transfer area (A) must be higher than the required area, according to a design excess area parameter $\hat{X}a$:

$$\hat{X}a \le \frac{A}{Areq} \tag{19}$$

where:

$$A = NbayNbbayNrNtrAotL \tag{20}$$

2.4. Geometric constraints

The tube pitch must allow a minimum gap between adjacent fin tips ($\widehat{\alpha t}$):

$$Ltp \ge Df + \widehat{\alpha t} \tag{21}$$

The area of the fans must be at least 40 percent of the heat exchanger face area and the fan diameters must be circumvented in the bay limits:

$$\frac{\pi}{4}NfanbayDfan^2 \ge 0.4NbbayWL \tag{22}$$

$$NbbayW \ge Dfan + 2\hat{f}d \tag{23}$$

$$Dfan + 2\hat{f}l \le L - Lfanp(Nfanbay - 1) \tag{24}$$

Additionally, the gap between fan rings is defined as 10% of the fan diameter:

$$Lfanp = 1.1Dfan \tag{25}$$

According to the validation range of the tube-side heat transfer correlation, the tube length must be longer than 10 diameters:

$$\frac{L}{Dti} \ge 10 \tag{26}$$

Additionally, according to the air heat transfer correlation, the following bounds are added:

$$Nr \ge 3 \tag{27}$$

$$0.011176 \text{ m} \le Dte \le 0.0508 \text{ m} \tag{28}$$

$$0.00584 \text{ m} \le Lf \le 0.0191 \text{ m} \tag{29}$$

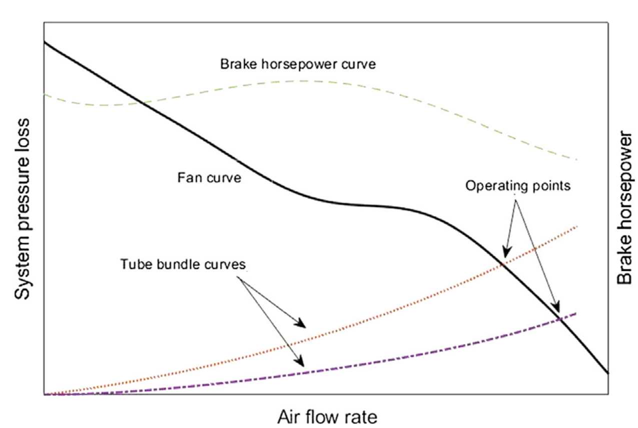

Fig. 2. Fan and tube bundle curves.

$$0.0274\ \text{m} \le Ltp \le 0.0986\ \text{m} \tag{30}$$

$$275 \le Nf \le 433 \tag{31}$$

$$1 \le \frac{Aot}{Ar} \le 50 \tag{32}$$

2.5. Reynolds number ranges

These limits are associated to the range of validity of the correlations [17]:

$$Reh \ge 10000 \tag{33}$$

$$1,800 \le Rec \le 100,000 \tag{34}$$

3. Objective function

The objective function is the total annualized cost (*TAC*), where capital (*Cinv*), maintenance (*Cmai*) and operational costs (*Cop*) are added:

$$TAC = C\hat{R}FCinv + Cmai + Cop \tag{35}$$

Each term of the objective function is taken form Conradie et al. [18] (see Supplementary Material).

4. Optimization procedures

Computational tests of the solution of the design problem through mathematical programming using local solvers (DICOPT and SBB) indicated that the convergence depends on good initialization, so close to the optimum that it amounts to knowing the solution already. The utilization of a global solver (BARON) did not found a feasible solution. Thus, instead of using MINLP solvers, we proposed three procedures to search the space of potential configurations that identify the global optimum, as presented next.

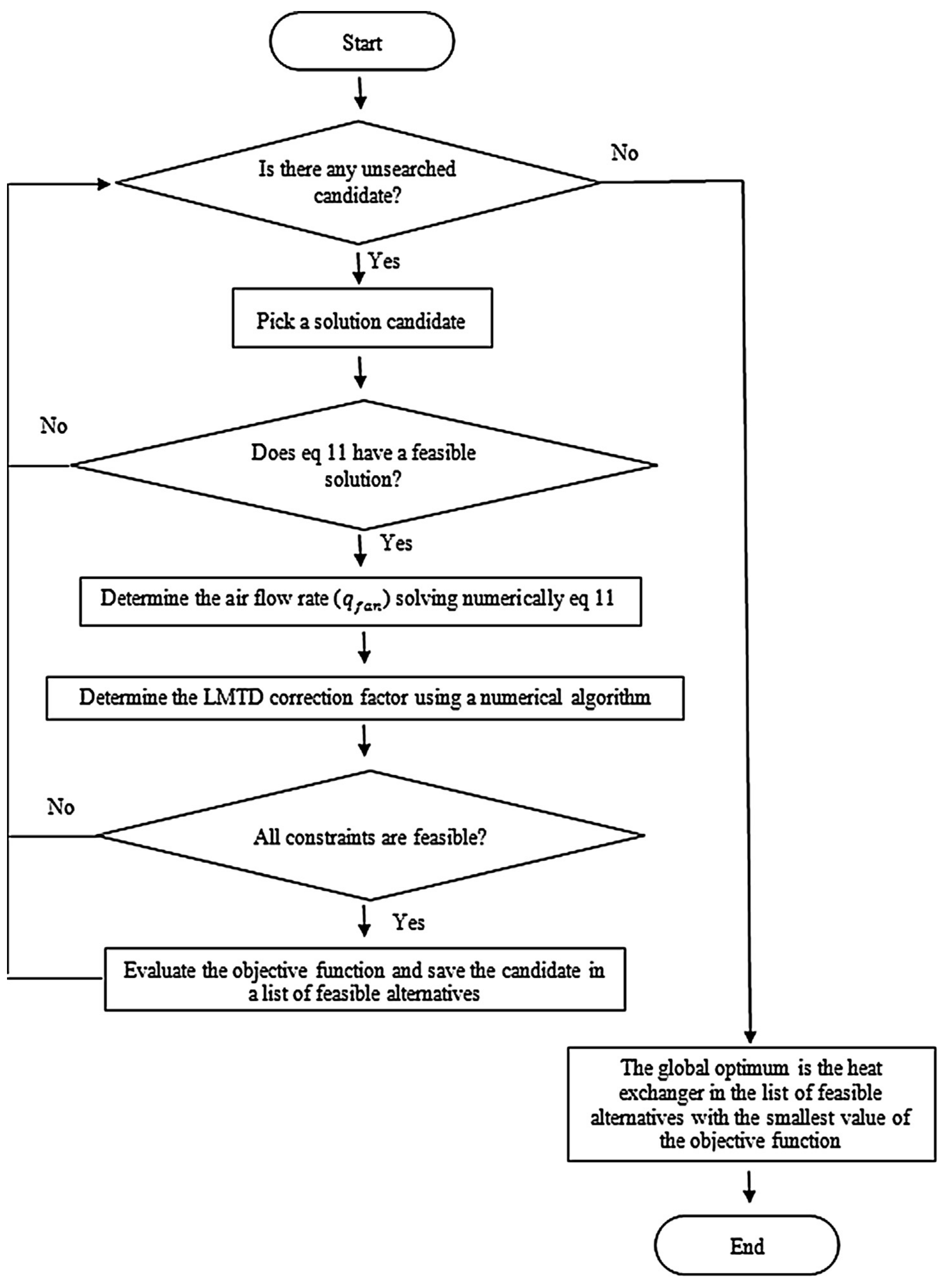

Fig. 3. Naïve exhaustive enumeration algorithm.

4.1. Search space

Each solution alternative is composed of a set of design variables, which are discrete in nature mostly due to their physical nature and/or commercially available options. Therefore, the search space corresponds to a table containing all possible combinations of the discrete values of the following design variables: (1) Finned tube commercial alternatives of diameter, fin diameter, number of fins per meter, and fin thickness; (2) Tube length; (3) Tube pitch ratio (ratio between the tube pitch and the outer tube diameter); (4) Number of bays; (5) Number of bundles per bay; (6) Number of tubes per row; (7) Heat exchanger configuration (combination of the number of rows and the number of tube passes); (8) Number of fans per bay; (9) Fan model (each associated to a specific fan diameter and fan curve).

4.2. Enumeration schemes

Three different enumeration schemes are described next:

- Naïve Exhaustive Enumeration: it consists of the feasibility check and cost calculation of all solution candidates of the search space (see Fig. 3). It has the highest computational effort and we use it only to compare the efficiency of the other searching schemes. (See Fig. 4.).
- Exhaustive Enumeration Preceded by Reduction of the Search Space: it aims at eliminating options that are not geometrically feasible first, to then solve the most computationally expensive hydraulic and thermal models.
- Smart enumeration: it is based on a search of the alternatives organized by increased order of capital and maintenance costs, determining hydraulic and thermal feasibility, and using an additional stopping criterion, that is, when the current capital and maintenance cost is larger than the total cost of the incumbent solution the algorithm stops (see Fig. 5 and Fig. 6). Because of the prior reordering, no solution can be found that has lower cost.

All the above procedures identify the global optimum. Exhaustive enumeration does it by construction, while smart enumeration does it

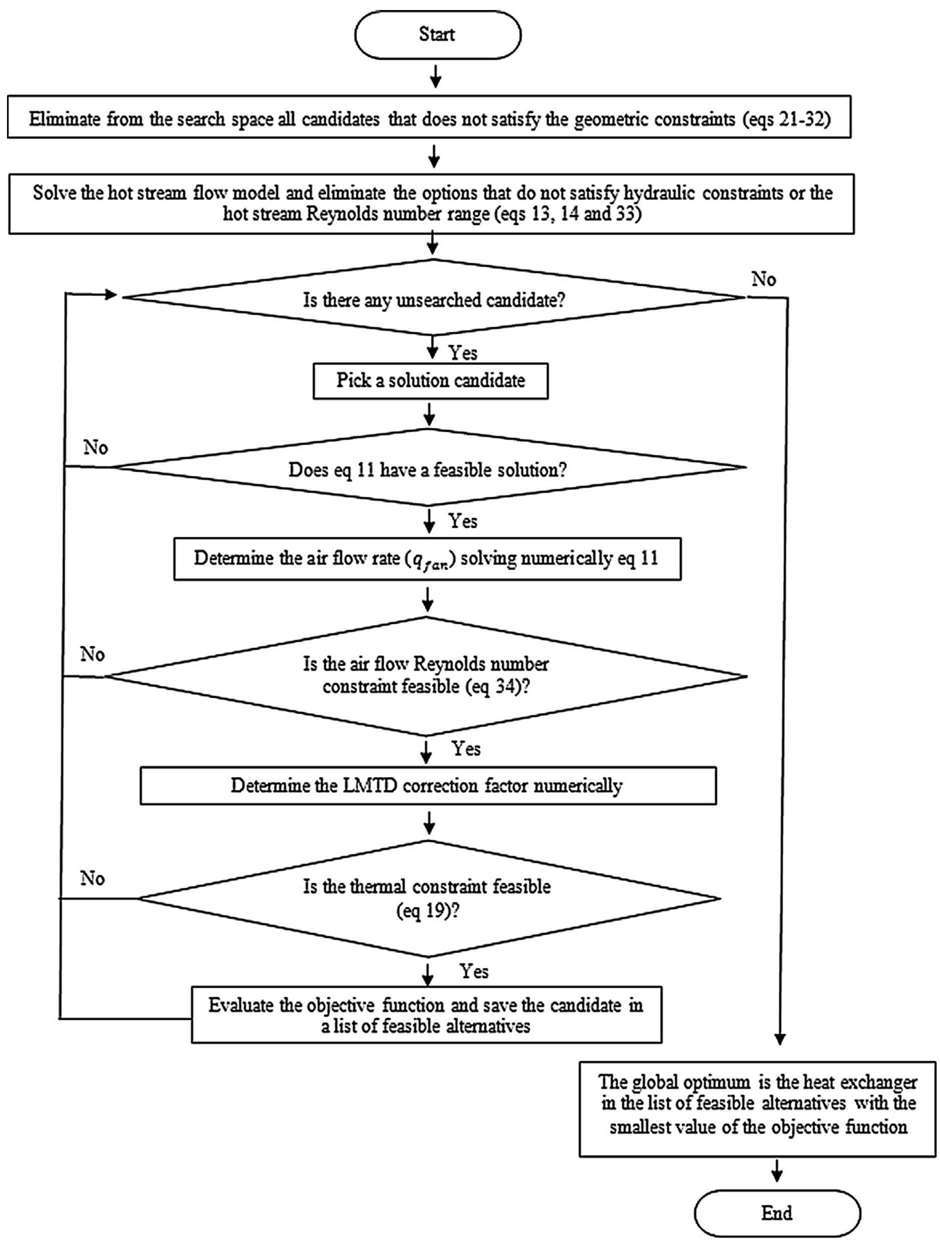

Fig. 4. Exhaustive enumeration preceded by reduction of the search space.

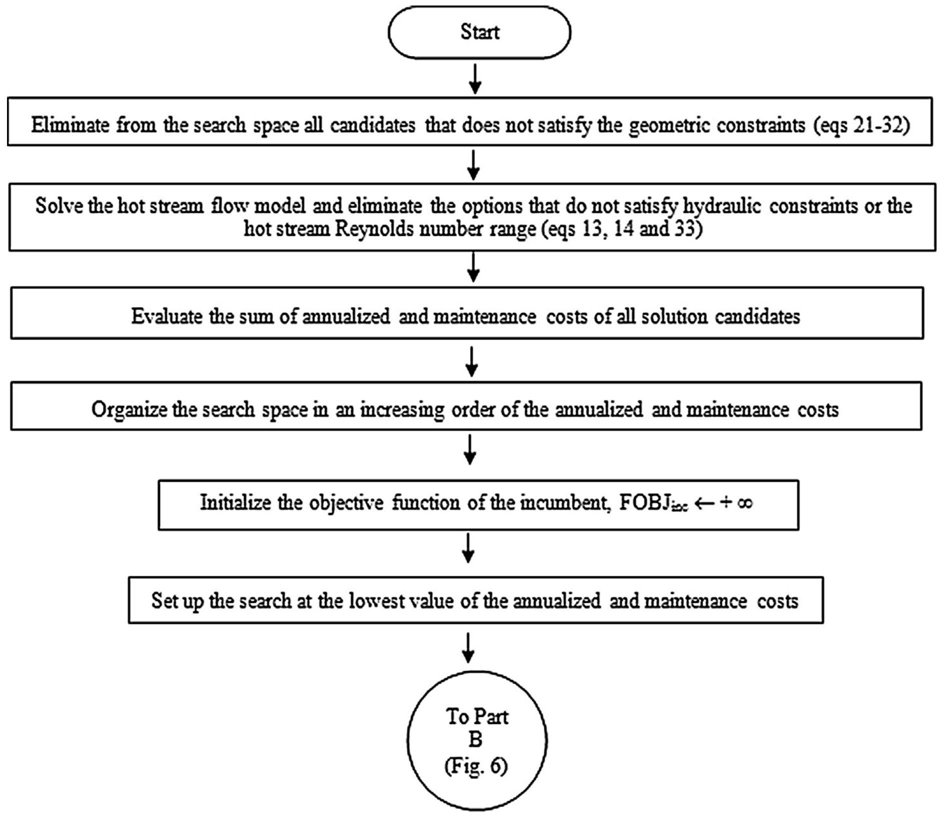

Fig. 5. Smart enumeration algorithm – Part A.

by construction and the use of the stopping criteria.

4.3. Analysis of a solution candidate

The enumeration procedures involve an analysis of solution candidates along the search path, in order to verify its feasibility and determine the corresponding value of the objective function.

A feasible solution must comply with the following set of constraints:

- Thermal constraints: Eq. (19);
- Hydraulic constraints: Eqs. (13) and (14);
- Geometric constraints: Eqs. (21)–(32);
- Reynolds number ranges: Eqs. (33) and (34).

The analysis of the thermal and hydraulic constraints demands the solution of the thermofluid dynamic model of the heat exchanger. The flow model (Eq. (11)) must be solved numerically to obtain the air flow rate. Next, the thermal model is solved, where the LMTD correction factor (F) is obtained numerically in the same way as in Souza et al. [7] (see Supplementary material).

Both nonlinear equations were solved using the trust region reflective least squares algorithm available on Matlab. A feasibility test between system and fan curves is performed prior to the solution procedure, where maximum and minimum pressure drops allowable by the fan must include the range of the pressure drop across the tube bundle curves. The operational range of all fans considered in this work is monotone and, if Eq. (11) has a solution, it is unique.

5. Results

The search algorithms were implemented in Matlab® R2018a, using an Intel® Core i7 3.6 GHz processor, with an 8 GB RAM memory. The proposed model was validated through the reproduction of the results reported by Souza et al. [7] (Example 1 described below).

Two examples are discussed below, further details of the input data and the corresponding results can be found in the Supplementary Material.

5.1. Example 1

The data are taken from Serth [17] (see Table 1).

The search space of design variables and economic data are equal to those presented by Souza et al. [7], expanded here by adding seven alternatives of fan options (see Supplementary Material). The total number of solution candidates is 302,400.

Table 2 reports the optimal values obtained. Because the air flow rate is varied, the model also calculates the air outlet temperature

The value of the objective function obtained is about 25% smaller than the air cooler reported by Serth [17] and 8.5% smaller than the value obtained by Souza et al. [7]. However, the comparison with Souza et al. [7] must consider that: (a) in our case the fan efficiency depends on the fan option, while Souza et al. [7] employed a constant value (0.70); (b) the air flow rate in Souza et al. [7] is defined by the user, so there is no guarantee that a fan model able to supply this air flow rate exists, requiring some rounding up of the air flow rate to a value of a commercial fan. The solution is thus sub-optimal even for the fixed air flow model they use.

The importance of including the air flow rate in the optimization is illustrated in Fig. 7. This graph shows the solution of Souza et al. [7] for different values of air flow rates (the dashed line is an interpolation curve). In Fig. 7a, it is possible to observe the large variation of the optimal objective function along the air flow rate range. Additionally, Fig. 7a also illustrates that Souza et al. [7] solution (130.15 kg/s) is near the optimal value of the air flow rate (140.12 kg/s) for the present model, explaining the proximity of the objective functions Had other flows been selected by Souza et al. [7] the differences would have been more pronounced. Another aspect that must be considered is the

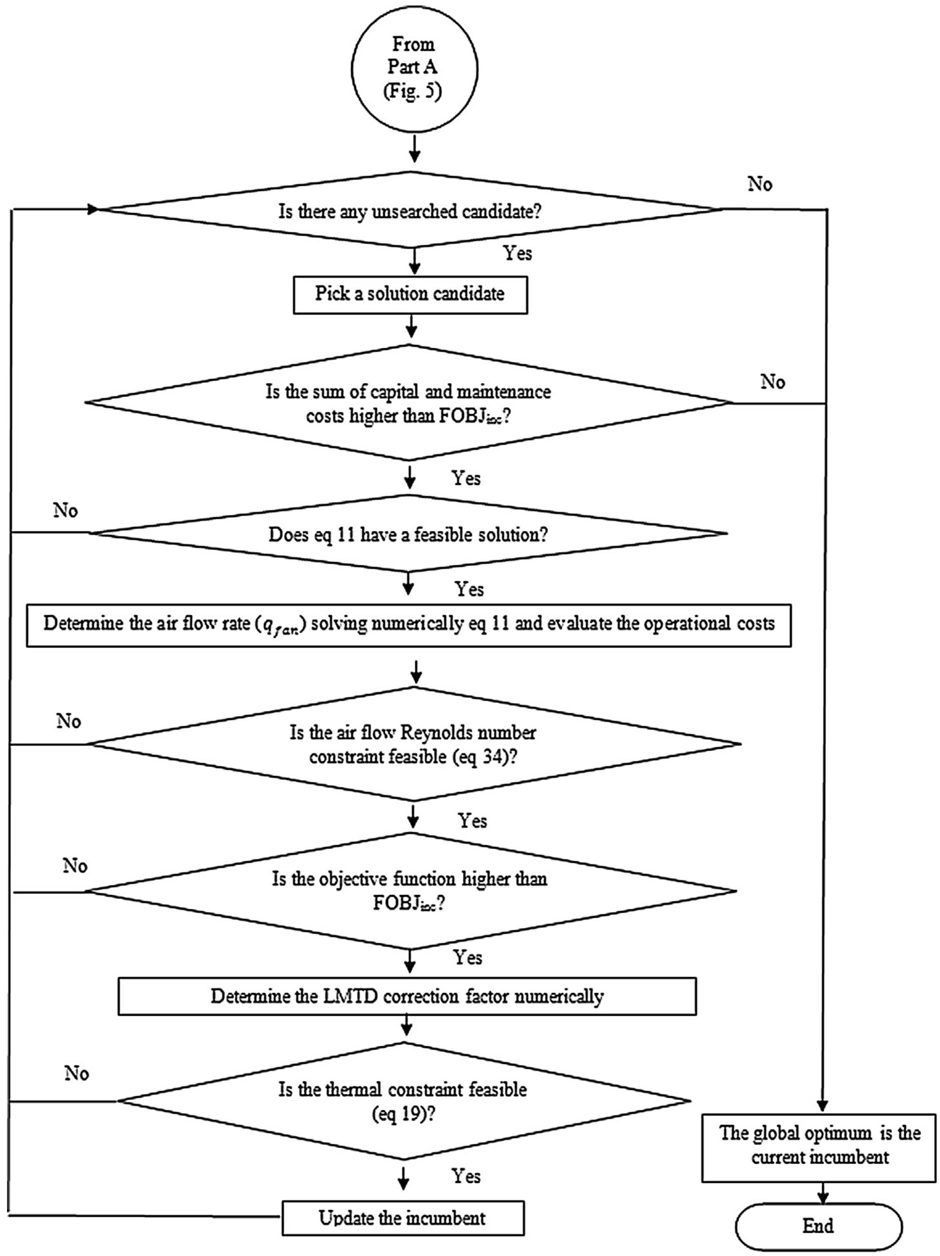

Fig. 6. Smart enumeration algorithm – Part B.

Table 1
Problem data.

	Tube side	Air side
Fluid	Hydrocarbon	Air
Mass flow rate (kg/s)	31.5	–
Inlet temperature (°C)	121.15	35.05
Outlet temperature (°C)	65.65	–
Fouling factor (m^2 K/W)	$1.7611 \cdot 10^{-4}$	0
Allowable pressure drop (Pa)	105,000	–
Flow velocity bounds (m/s)	1–3	–
Reynolds bounds	10,000 -	1,800–10^5
Density (kg/m^3)	800	Supplementary Material
Thermal conductivity (W/(m·K))	0.14	Supplementary Material
Heat capacity (J/(kg·K))	2303	Supplementary Material
Viscosity (Pa·s)	$5 \cdot 10^{-4}$	Supplementary Material

Table 2
Example 1: Optimal Design Variables.

Variable	This article	Souza et al. [7]	Serth [17]
Area (m^2)	5631	6307	4181
Capital Cost ($/year)	19,125	23,553	16,317
Maintenance Cost ($/year)	2838	1499	1092
Operational Cost ($/year)	5279	4759	19,422
Total Annualized Cost ($/year)	27,242	29,811	36,830

nonconvex profile of the optimal values of the objective function. This pattern is better visualized through Fig. 7b, which depicts a narrow range around the minimum.

5.1.1. Computational performance

The naïve exhaustive enumeration elapsed time was 7,390 s. The application of the prior reduction of the search space reduced the elapsed time to 206 s. Finally, the smart enumeration brought an

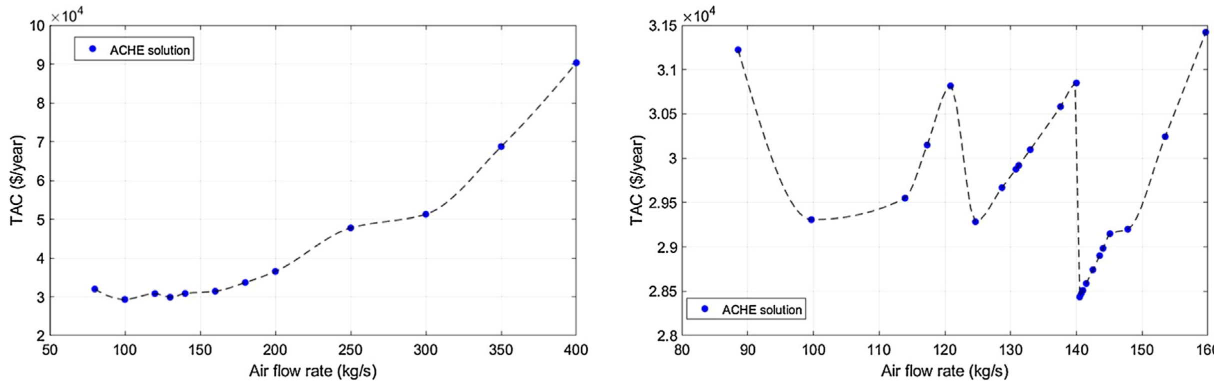

Fig. 7. Variation of the TAC of the air cooler design problem in relation to the air flow rate.

additional reduction, an elapsed time of 141 s.

The prior reduction of the search space shows a reduction of 93.8% of the computational time because the exhaustive enumeration solves the two nonlinear equations of all 302,400 problems, Indeed, the number of nonlinear problems to be solved is reduced to 8,714 options for the hydraulic model and 1,885 options for the thermal model. The smart enumeration shows an additional reduction of 31.5% in relation to the previous alternative: the number of nonlinear problems solved is reduced to 8,380 for the hydraulic model (2.77% of the total solution candidates) and 1,391 for the thermal model (0.46% of the total of solution candidates).

5.2. Example 2

The second example considers a larger search space using the smart enumeration procedure (see Supplementary Material). The physical properties of the streams are the same of the data presented in Table 1 and the problem consists in cooling 90.15 kg/s of the process stream from 210 °C to 104 °C with air at 35.05 °C.

The number of geometry options is 3,333,960 (i.e. about 11-fold increase of the dimension of the search space compared to Example 1). The remaining input data are the same.

For this case, both prior reduction and smart search algorithm found the total annualized cost of 79,205 $/year. The prior reduction of search space algorithm took 3,540 s and the smart enumeration scheme took 1,609 s to find the global optimum, i.e. the smart search was twice faster than the prior reduction. Despite the large increase of the dimension of the search space, the necessary computational time is still acceptable for the application of the proposed procedure for the solution of real design problems.

6. Conclusions

A modeling of an air-cooled heat exchanger unit was presented that includes the selection of a commercial fan. For this, a fluid dynamic model of the hydraulic interactions between fans and tube bundles was developed. The global solution of the problem was obtained using three variants of enumeration schemes, aiming at reducing the numerical effort.

Based on a literature example where the air flow is a-priori fixed, it was possible to reduce costs, thus illustrating the need to include this variable in the optimization. The comparison of the performance of the enumeration schemes for the same example indicated that the smart enumeration brought a considerable computational effort reduction. The main features of the smart enumeration scheme which allowed the reduction of the computational effort are: (a) prior reduction of the search space, eliminating a large set of infeasible candidates without solving them; (b) utilization of an incumbent, which represents the best solution obtained during the search, to accelerate the identification of the global solution; (c) organization of the set of feasibility tests in an organized fashion aiming at reducing the number of nonlinear problems solved; (d) inclusion of a stopping criterion based on the incumbent that is identified as one that cannot be improved. Finally, the application of the smart enumeration procedure to another example, associated to a large search space, indicated the potentiality of the proposed approach for solving real problems.

Acknowledgements

Carolina B. de Carvalho thanks the Coordination for the Improvement of Higher Education Personnel (CAPES) for the doctoral fellowship. André L. H. Costa and Mauro A. S. S. Ravagnani thank the National Council for Scientific and Technological Development (CNPq), for the research productivity fellowship. André L. H. Costa thanks the Rio de Janeiro State University (UERJ) by the financial support through the Prociência Program.

Appendix A. Supplementary material

Supplementary data to this article can be found online at https://doi.org/10.1016/j.applthermaleng.2019.114188.

References

[1] A.R. Doodman, M. Fesanghary, R. Hosseini, A robust stochastic approach for design optimization of air cooled heat exchangers, Appl. Energy. 86 (2009) 1240–1245.
[2] A. Karami, E. Rezaei, M. Shahhosseni, M. Aghakhani, Optimization of heat transfer in an air cooler equipped with classic twisted tape inserts using imperialist competitive algorithm, Exp. Therm. Fluid Sci. 38 (2012) 195–200.
[3] E. Rezaei, M. Karami, M. Alimohammad Shahhosseni, Aghakhani, The optimization of thermal performance of an air cooler equipped with butterfly inserts by the use of imperialist competitive algorithm, Heat Transf. Res. 41 (2012) 214–226.
[4] A. Hesam, A. Kashani, A. Maddahi, H. Hajabdollahi, Thermal-economic optimization of an air-cooled heat exchanger unit, Appl. Therm. Eng. 54 (2013) 43–55.
[5] M. Gonzalez, N. Petracci, M. Urbicain, Air-cooled heat exchanger design using successive quadratic programming (SQP), Heat Transf. Eng. 22 (2001) 11–16.
[6] J. Ma, Y. Wang, X. Feng, D. Xu, Synthesis cooling water system with air coolers, Chem. Eng. Res. Des. 131 (2018) 643–655.
[7] P.A. Souza, A.L.H. Costa, M.J. Bagajewicz, Globally optimal linear approach for the design of process equipment: the case of air coolers, AIChE J. 64 (2018) 886–903.
[8] W.F. He, Y.P. Dai, J.F. Wang, M.Q. Li, Q.Z. Ma, Performance prediction of an air-cooled steam condenser using UDF method, Appl. Therm. Eng. 50 (2013) 1339–1350.
[9] W. He, D. Han, C. Yue, W. Pu, Y. Dai, Mechanism of the air temperature rise at the forced draught fan inlets in an air-cooled steam condenser, Appl. Therm. Eng. 71 (2014) 355–363.
[10] L. Chen, L. Yang, X. Du, Y. Yang, Anti-freezing of air-cooled heat exchanger by air flow control of louvers in power plants, Appl. Therm. Eng. 106 (2016) 537–550.
[11] X. Li, N. Wang, L. Wang, I. Kantor, J.-L. Robineau, Y. Yang, F. Maréchal, A data-driven model for the air-cooling condenser of thermal power plants based on data reconciliation and support vector regression, Appl. Therm. Eng. 129 (2018) 1496–1507.
[12] M.F.M. Fahmy, H.I. Nabih, Impact of ambient air temperature and heat load

variation on the performance of air-cooled heat exchangers in propane cycles in LNG plants – analytical approach, Energy Convers. Manag. 121 (2016) 22–35.

[13] H. Reuter, N. Anderson, Performance evaluation of a bare tube air-cooled heat exchanger bundle in wet and dry mode, Appl. Therm. Eng. 105 (2016) 1030–1040.

[14] Y. Kong, W. Wang, L. Yang, X. Du, Y. Yang, A novel natural draft dry cooling system with bilaterally arranged air-cooled heat exchanger, Int. J. Therm. Sci. 112 (2017) 318–334.

[15] L. Chen, L. Yang, X. Du, Y. Yang, A novel layout of air-cooled condensers to improve thermo-flow performances, Appl. Energy. 165 (2016) 244–259, https://doi.org/10.1016/j.apenergy.2015.11.062.

[16] R. Al-Waked, M. Behnia, The effect of windbreak walls on the thermal performance of natural draft dry cooling towers, Heat Transf. Eng. 26 (2005) 50–62.

[17] R.W. Serth, Process heat transfer: principles and applications, 1st ed.,, Elsevier Ltd., 2007.

[18] A.E. Conradie, J.D. Buys, D.G. Kroger, Performance optimization of dry-cooling systems for power plants through SQP methods, Appl. Therm. Eng. 18 (1998) 25–45.